

General mechanism for orbital selective phase transitions

Yu-Zhong Zhang,^{1,*} Hunpyo Lee,² Hai-Qing Lin,³ Chang-Qin Wu,⁴ Harald O. Jeschke,² and Roser Valentí²

¹Shanghai Key Laboratory of Special Artificial Microstructure Materials and Technology, & Physics Department, Tongji University, Shanghai 200092, P.R. China

²Institut für Theoretische Physik, Goethe-Universität Frankfurt, Max-von-Laue-Strasse 1, D-60438 Frankfurt/Main, Germany

³Beijing Computational Science Research Center, Beijing 100084, China

⁴Department of Physics and State Key Laboratory of Surface Physics, Fudan University, Shanghai 200433, China

(Received 8 November 2011; revised manuscript received 8 January 2012; published 26 January 2012)

Based on the analysis of a two-orbital Hubbard model within a mean-field approach, we propose a mechanism for an orbital selective phase transition (OSPT) where coexistence of localized and itinerant electrons can be realized. We show that this OSPT exists both at and near half-filling even in the absence of crystal-field splittings or when bandwidths, orbital degeneracies, and magnetic states are equal for both orbitals, provided the orbitals have different band dispersions. Such conditions should generally be satisfied in many materials. We find that this OSPT is not sensitive to the strength of Hund's rule coupling and that heavy doping favors the collinear antiferromagnetic state over the OSPT. We discuss our results in relation to the iron pnictides.

DOI: 10.1103/PhysRevB.85.035123

PACS number(s): 71.10.Fd, 71.10.Hf, 71.30.+h, 75.10.-b

I. INTRODUCTION

Orbital selective phase transitions (OSPTs) leading to phases where localized and itinerant electrons coexist have attracted extensive interest from both experimentalists¹⁻⁶ and theoreticians⁷⁻²⁴ since the observation in the metallic phase of $\text{Ca}_{2-x}\text{Sr}_x\text{RuO}_4$ ($0.2 \leq x \leq 0.5$) of an anomalous behavior with a Curie-Weiss-like local spin.²⁵ Despite the controversies regarding the applicability of such a proposal to real compounds,²⁶⁻²⁸ various mechanisms for OSPTs have been investigated, such as two orbitals with different bandwidths at half-filling,⁷⁻²² away from half-filling with crystal-field splitting,²⁹ the coexistence of different orbital degeneracies with crystal-field splitting at any filling,³⁰ and different magnetic states in different orbitals at half-filling.³¹

Recently, various models based on the assumption of the coexistence of localized and itinerant electrons have been proposed in order to describe the magnetism in the new iron-based superconductors.³²⁻³⁸ Less work has been done on understanding the origin of such orbital selective phases (OSPs). As one possible mechanism for the OSPTs in pnictides, bands with similar bandwidths having different intraband Coulomb repulsions were suggested in analogy to the mechanism of a difference in bandwidth.³⁹ However, since most previous studies on the origin of OSPs are focused on the paramagnetic (PM) state, a correct description of the magnetism observed in the parent compounds of most iron pnictides calls for a reinvestigation of the mechanism responsible for OSPs with magnetic order.

In this paper, a possible OSPT mechanism is proposed based on a simple two-dimensional (2D) two-orbital Hubbard model with both orbitals having different band dispersions. We solve the model in the context of mean-field theory [Hartree-Fock approximation (HFA)]. A comparison of our results to those obtained from the dynamical mean-field approximation (DMFA) at and near half-filling shows that OSPTs can be qualitatively captured already at the mean-field level without taking dynamical fluctuations into account. The advantage of working with the mean-field approach is that we are able to investigate a large variety of cases not easily accessible within

the DMFA. We show that even in the absence of crystal-field splittings or when bandwidths, orbital degeneracies, magnetic states, and intra-band Coulomb repulsions are equal for both orbitals, OSPTs can still occur at different band fillings. We show that it is the distinct band dispersion in both orbitals that can be identified as the crucial ingredient for the presence of OSPTs with magnetic order. The mechanism we consider is in fact very general since usually the strength of hybridizations between neighboring sites in different directions is strongly orbital dependent in real materials, leading to distinct band dispersions in different orbitals.

II. MODEL AND METHOD

The 2D two-orbital Hubbard model is defined as

$$H = - \sum_{\langle ij \rangle, \langle\langle ij \rangle\rangle, \gamma\sigma} t_{ij,\gamma} c_{i\gamma\sigma}^\dagger c_{j\gamma\sigma} + U \sum_{i\gamma} n_{i\gamma\uparrow} n_{i\gamma\downarrow} + \left(U' - \frac{J}{2} \right) \sum_{i\gamma>\gamma'} n_{i\gamma} n_{i\gamma'} - 2J \sum_{i\gamma>\gamma'} S_{i\gamma} \cdot S_{i\gamma'}, \quad (1)$$

where $t_{ij,\gamma} = t_\gamma (t'_\gamma)$ is the intraorbital hopping integral between nearest-neighbor (NN) (next-nearest-neighbor (NNN)) sites denoted $\langle ij \rangle$ ($\langle\langle ij \rangle\rangle$), with band indices $\gamma = \alpha, \beta$ in units of t . U , U' , and J are the intraband Coulomb interaction, interband Coulomb interaction, and Hund's coupling, respectively, which fulfill the rotational invariance condition $U = U' + 2J$. The pair-hopping term is ignored, as it does not affect our mean-field results.⁴⁰⁻⁴³ $c_{i\gamma\sigma}^\dagger$ ($c_{i\gamma\sigma}$) creates (annihilates) an electron in orbital γ of site i with spin σ . $n_{i\gamma\sigma}$ is the occupation operator, while $n_{i\gamma} = n_{i\gamma\uparrow} + n_{i\gamma\downarrow}$, and $S_{i\gamma}$ is the spin operator.

In order to access the true ground state in a 2D system with hoppings up to NNN sites, the original lattice is divided into two sublattices, A and B [see Fig. 1(a)], allowing us to consider various magnetic states in uniform formulation, such as the PM state, ferromagnetic (FM) state with momentum $Q_{A/B,\gamma} = (0,0)$ and magnetization $m_{A,\gamma}^{x/y} = m_{B,\gamma}^{x/y}$, Néel antiferromagnetic (NAF) state with $Q_{A/B,\gamma} = (0,0)$ and $m_{A,\gamma}^{x/y} = -m_{B,\gamma}^{x/y}$, collinear antiferromagnetic (CAF) state

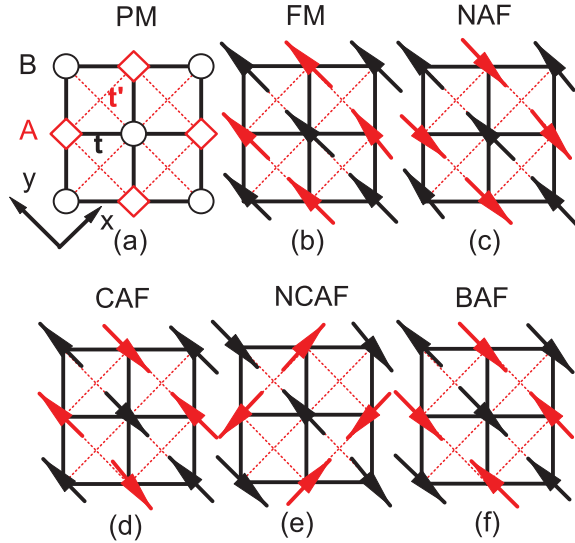


FIG. 1. (Color online) Schemes for the different magnetically ordered states we use in our calculations. (a) Paramagnetic state. Choices of sublattice and coordinate system are shown. (b) Ferromagnetic, (c) Néel, (d) collinear, (e) noncollinear, and (f) bicollinear antiferromagnetic states.

with $Q_{A/B,\gamma} = (\pi, \pi)$ and $m_{A,\gamma}^{x/y} = m_{B,\gamma}^{x/y}$, bicollinear AF state with $Q_{A/B,\gamma} = (0, \pi)$ and $m_{A,\gamma}^{x/y} = m_{B,\gamma}^{x/y}$, and noncollinear AF (NCAF) state with $Q_{A/B,\gamma} = (\pi, \pi)$ and $m_{A,\gamma}^{x/y} = m_{B,\gamma}^{y/x}$,⁴⁰ where $|m_{i,\gamma}| = |m_{i,\gamma}^x + im_{i,\gamma}^y| = |\frac{1}{N} \sum_k (c_{ki\gamma\uparrow}^\dagger c_{k+Q_{i\gamma}\downarrow})|$ with $i = A$ or B . The corresponding schemes for different magnetic patterns are shown in Figs. 1(a)–1(f).

III. COMPARISONS BETWEEN HFA AND DMFA RESULTS

In order to check the validity of our mean-field calculations, we first compare our results with those obtained using the DMFA.^{44–46} For this comparison, the chemical potential rather than the filling is fixed, as is usually done in DMFA studies, and only the NAF state is allowed, as required by a two-sublattice calculation within the DMFA.⁴⁷ Figure 2(a) shows the sublattice magnetization as a function of interaction U/t for the cases $t_\alpha = 1$, $t'_\alpha = 0.6$, and $t_\beta = 1$, $t'_\beta = 0$. We find that while the magnetic phase transition obtained from the HFA happens earlier than that from the DMFA and higher magnetization is detected in the HFA—indicating that dynamical fluctuations ignored in the HFA strongly suppress the magnetically ordered states—the variation of the magnetization with U/t obtained from the DMFA can be qualitatively reproduced by the results from the HFA. Furthermore, all phases given from the DMFA can be qualitatively captured by the HFA as shown in Figs. 2(b)–2(d) and 2(e)–2(g), which depict the density of states (DOS) in the different phases obtained from the DMFA and HFA, respectively. The OSPT, where one orbital becomes localized while the other remains metallic, is clearly detected by both the DMFA [Fig. 2(c)] and the HFA [Fig. 2(f)]. The resulting OSP is sandwiched between the PM metallic state and the NAF insulating state as shown in Figs. 2(b) and 2(d) for the DMFA and Figs. 2(e) and 2(g) for the HFA. The qualitative consistency between the results from the HFA and

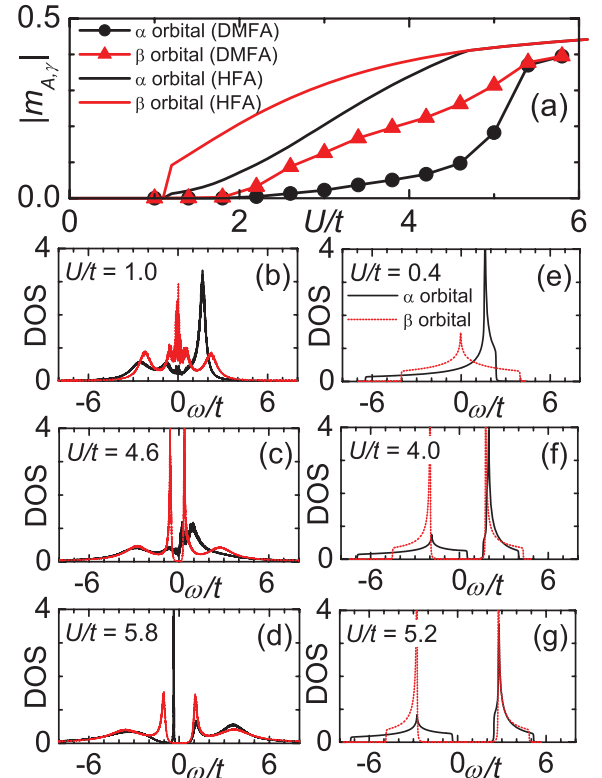


FIG. 2. (Color online) Comparison of results from the Hartree-Fock approximation (HFA) versus the dynamical mean-field approximation (DMFA) at $t_\alpha = 1$, $t'_\alpha = 0.6$, $t_\beta = 1$, $t'_\beta = 0$, and $J/U = 0.25$. (a) Magnetization as a function of U/t . Density of states in different phases from (b)–(d) the DMFA and (e)–(g) the HFA.

those from the DMFA imply the validity of our following discussion on the OSP as well as on other phases in our model at the mean-field level. In fact, it is already known from the DMFA—where spatial fluctuations are absent—that the PM metal-insulator transition, which is inaccessible to the HFA, is precluded by a magnetic phase transition in the half-filled case at zero temperature,⁴⁸ which may be qualitatively described by the HFA. Comparing the DMFA and HFA on other hopping parameters with different t'_α (not shown here), we conclude that dynamical fluctuations play a minor role in the OSPT.

IV. THE GENERAL MECHANISM FOR OSPT

In the following we investigate the case of fixed filling at $1/2$, in contrast to the case of a fixed chemical potential, where the filling is changed as a function of interaction U/t . All the magnetically ordered states shown in Fig. 1 are taken into account and the ground state is the one with the lowest total energy. Figure 3(a) shows the phase transitions happening at $t_\alpha = 1$, $t'_\alpha = 0.8$ and $t_\beta = 1$, $t'_\beta = 0$ as a function of U/t . As long as $U/t < 2.88$, the ground state is a PM metal with orbital order. In the small interaction region of $2.88 < U/t < 3.08$, a NAF metal with orbital order appears. Upon further increasing U/t , from 3.08 up to 4.02, the α orbital exhibits NAF insulating behavior while the β orbital remains in the NAF metallic state, indicating an OSP. Orbital order disappears

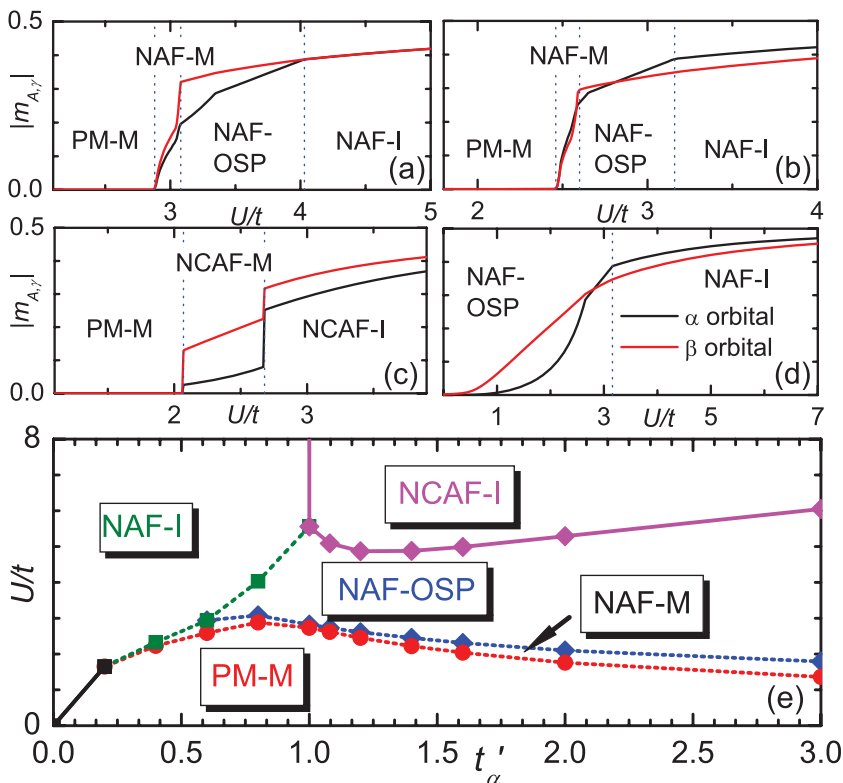


FIG. 3. (Color online) Variation of the magnetization as a function of U/t (a) at $t_\alpha = 1$, $t'_\alpha = 0.8$, and $t_\beta = 1$, $t'_\beta = 0$; (b) at $t_\alpha = 0.769$, $t'_\alpha = 0.615$, and $t_\beta = 1$, $t'_\beta = 0$; (c) at $t_\alpha = 1$, $t'_\alpha = 0.8$ and $t_\beta = 0.769$, $t'_\beta = 0.615$; (d) after eliminating the orbital order by adding an effective crystal-field splitting of $\Delta = 0.798$ at $t_\alpha = 0.769$, $t'_\alpha = 0.615$ and $t_\beta = 1$, $t'_\beta = 0$, where the term for crystal-field splitting is written as $\sum_i \Delta(n_{i\beta} - n_{i\alpha})$. (e) Phase diagram in $U/t-t'_\alpha$ at $t_\alpha = 1$, $t_\beta = 1$, $t'_\beta = 0$. Here $J/U = 0.25$ and filling is $1/2$. Regions of different phases are indicated by the abbreviations defined in the text. M, metal; I, insulator. Solid and dotted lines represent first- and second-order phase transitions, respectively.

in this interaction region. At $U/t > 4.02$, both orbitals display NAF insulating behavior.

Though we have demonstrated that the OSPT is still present at fixed filling in finite dimension, the mechanism for it has not yet been identified. After analyzing the noninteracting DOS, we find that several possible mechanisms coexist, such as (i) two orbitals having different bandwidths with the ratio $W_\alpha/W_\beta = 1.3$; (ii) the existence of orbital order due to the different band dispersions of the two orbitals ($t'_\alpha/t_\alpha \neq t'_\beta/t_\beta$), which can be viewed as the existence of an effective crystal-field splitting; and (iii) two orbitals having distinct band dispersions, which leads to different shapes of the noninteracting partial DOS. The last effect was not considered in previous DMFA studies, where a semicircular DOS with particle-hole symmetry has usually been employed for all the orbitals.

In order to figure out the essential mechanism responsible for the OSPT observed above, we study three cases separately. (i) First, we eliminate the effect of different bandwidths by rescaling the hopping parameters of the α orbital from $t_\alpha = 1$, $t'_\alpha = 0.8$ to $t_\alpha = 0.769$, $t'_\alpha = 0.615$ so that the ratio of $t'_\alpha/t_\alpha = 0.8$ is retained while the ratio of bandwidths becomes $W_\alpha/W_\beta = 1$. Figure 3(b) presents the various phases as a function of U/t after rescaling. Though the critical points are changed due to the change in the total bandwidths, all the phases involving OSP are preserved, indicating that such an OSPT exists in the absence of bandwidth differences between orbitals.

(ii) In the second case we remove the orbital order by adding an effective crystal-field splitting, by which the half-filling condition is simultaneously satisfied at $U/t = 0$ in both

orbitals. Figure 3(d) shows that the OSPT is still present in the absence of orbital order. However, states with metallic behavior in both orbitals vanish since the Fermi level is located right at the van Hove singularity in the β orbital at $U/t = 0$. We have checked that a small t'_β , which shifts the van Hove singularity away from the Fermi level, leads to the appearance of metallic phases in both orbitals at finite U/t .

(iii) As a third option, we eliminate the effect of orbitals having distinct band dispersions but retain the difference in bandwidth by choosing $t_\alpha = 1$, $t'_\alpha = 0.8$ and $t_\beta = 0.769$, $t'_\beta = 0.615$ which leads to $t'_\alpha/t_\alpha = t'_\beta/t_\beta = 0.8$ and $W_\alpha/W_\beta = 1.3$. As shown in Fig. 3(c), an OSP is precluded by NCAF states, resulting in only two successive phase transitions from PM metals to NCAF insulators through NCAF metals in both orbitals. Clearly, the OSP will be replaced by NAF insulating states in both orbitals at any finite U/t if we take $t_\alpha = 1$, $t'_\alpha = 0$ and $t_\beta = 1.3$, $t'_\beta = 0$, which means a similar dispersion relation $t'_\alpha/t_\alpha = t'_\beta/t_\beta = 0$ but different bandwidth $W_\alpha/W_\beta = 1.3$, since the Fermi level crosses the van Hove singularities in both orbitals.

Our results so far strongly point to the fact that orbitals with distinct band dispersions are crucial for the OSPT since it is present even though all the other mechanisms mentioned above are absent while different bandwidths alone will not support the existence of OSPT when magnetic order is considered. Figure 3(e) presents a phase diagram in the $U/t-t'_\alpha$ plane at $t_\alpha = 1$, $t_\beta = 1$, and $t'_\beta = 0$. An OSP exists in a wide region of the phase diagram. The phase transitions from both NAF states to the NCAF state and from PM metal to NAF insulator are of first order (solid line) or, otherwise, second order (dotted line). The NAF metallic state has also been detected in the one-band Hubbard model with NN and NNN hoppings.⁴⁹

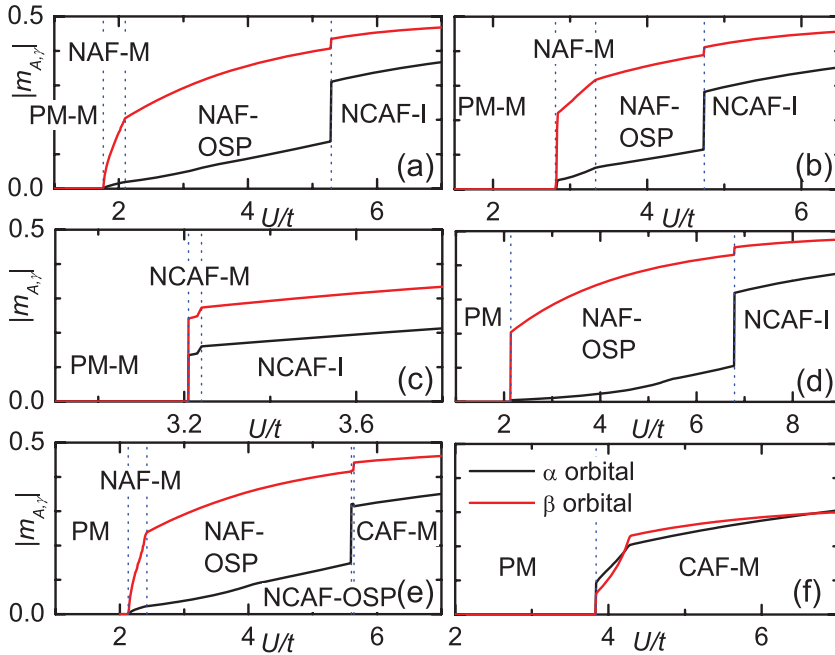


FIG. 4. (Color online) Variation of magnetization as a function of U/t at $t_\alpha = 1$, $t'_\alpha = 2$, $t_\beta = 1$. (a) $t'_\beta = 0$, $J/U = 0.25$; (b) $t'_\beta = 0.4$, $J/U = 0.25$; (c) $t'_\beta = 0.8$, $J/U = 0.25$; and (d) $t'_\beta = 0$, $J/U = 0.0625$ at half-filling. Electronic doping of (e) 2.5% and (f) 20% at $t'_\beta = 0$, $J/U = 0.25$. Regions of different phases are indicated by the abbreviations defined in the text. M, metal; I, insulator.

V. VARIOUS EFFECTS ON THE OBSERVED OSPT

Finally, we investigate various effects on the observed OSPT. From the phase diagram, it is obvious that we should discuss two cases separately: (i) $t'_\alpha/t_\alpha > 1$, where different magnetic orders, like NAF and NCAF orders, compete with each other; and (ii) $t'_\alpha/t_\alpha < 1$, where only NAF order occurs. In Fig. 4, we show the results at $t_\alpha = 1$, $t_\beta = 1$, and $t'_\alpha = 2$. We first present the effect of adding NNN hopping t'_β . It is found that increasing t'_β favors the NCAF state, which squeezes the region of the NAF OSP. As shown in Fig. 4(b), at $t'_\beta = 0.4$, the region of OSP is smaller than at $t'_\beta = 0$ [Fig. 4(a)], and at $t'_\beta = 0.8$ the OSP completely vanishes [see Fig. 4(c)]. However, for the case of $t'_\alpha = 0.8$ (not shown), the region of the OSP remains unchanged at $t'_\beta = 0.4$, while it is reasonably replaced by an NCAF state at $t'_\beta = 0.8$. The effect of Hund's rule coupling is presented in Fig. 4(d). Compared to Fig. 4(a), where $J/U = 0.25$, the region of OSP is enlarged, at $J/U = 0.0625$, and a direct first-order phase transition from PM metals in both orbitals to the NAF OSP is observed instead of two successive second-order phase transitions through an intermediate NAF metallic state at $J/U = 0.25$. For the case of $t'_\alpha = 0.8$, $t'_\beta = 0$ (not shown), a similar effect of the Hund's rule coupling is found.

Figure 4(e) shows that at the low concentration of electronic doping of 2.5%, the OSP with NAF order is slightly moved to higher values of U/t and the NCAF insulating states existing in the undoped case are replaced by a small region of OSP with NCAF order which eventually become CAF metallic states at larger U/t . At the high doping of 20%, only two phases with PM and CAF metallic states remain and the OSP vanishes as shown in Fig. 4(f). The critical value of doping concentration where the OSP disappears is around 13.6%. For the case of $t'_\alpha = 0.8$, $t'_\beta = 0$ (not shown), the OSPT also exists at 2.5% doping but is excluded by PM and CAF metallic states at 20% doping. It is interesting to note that CAF metallic

states only appear when the system is doped. Twenty percent electronic doping is related to the filling factor in the pnictides where six 3d electrons occupy five 3d orbitals. However, after examining various sets of model parameters, including those for the pnictides,^{41,50} we should emphasize that the OSPT disappears whenever CAF order occurs.

VI. DISCUSSION AND CONCLUSIONS

Recently, various efforts have been made to reconcile the controversies about the origin of the CAF phases observed in iron pnictides. Models containing coupled local spins and itinerant electrons have been proposed.^{32,34-38,51} Experimental data have also been interpreted in terms of the coexistence of local and itinerant electrons.^{52,53} However, such a compromise does not seem to be supported by the present study of OSPT with magnetic order. We find that OSPT and CAF order tend to avoid each other. Also, interorbital hoppings do not favor the OSP with CAF order. On the other hand, it is not to be expected that increasing the orbital degrees of freedom will dramatically change the situation. Furthermore, existing mechanisms proposed within the PM state are in conflict with the fact that the low-temperature phases of most pnictides are magnetically ordered, and the bandwidth of different orbitals are almost the same. However, quantum fluctuations, especially spatial rather than dynamical fluctuations, which favor PM states, may be responsible for possible OSPT in the pnictides.

In summary, we propose a general mechanism for an OSPT in magnetically ordered states. Different orbitals with different band dispersions should be quite widespread in real materials. Importantly, the OSPT according to the presented mechanism occurs over a wide range of model parameters, suggesting that this mechanism could be realized in nature.

ACKNOWLEDGMENTS

Y.Z. is supported by the National Natural Science Foundation of China (Grant No. 11174219), Shanghai Pujiang

Program (Grant No. 11PJ1409900), and Research Fund for the Doctoral Program of Higher Education of China (Grant No. 20110072110044). H.L. is supported by the DFG through

FOR 1346, and H.O.J. by the Helmholtz Association through Grant No. HA216/EMMI. Y.Z. is indebted to the CSRC for the hospitality from and partial financial support by the CAEP.

*yzzhang@tongji.edu.cn

- ¹S.-C. Wang, H.-B. Yang, A. K. P. Sekharan, S. Souma, H. Matsui, T. Sato, T. Takahashi, Chenxi Lu, Jiandi Zhang, R. Jin, D. Mandrus, E. W. Plummer, Z. Wang, and H. Ding, *Phys. Rev. Lett.* **93**, 177007 (2004).
- ²L. Balicas, S. Nakatsuji, D. Hall, T. Ohnishi, Z. Fisk, Y. Maeno, and D. J. Singh, *Phys. Rev. Lett.* **95**, 196407 (2005).
- ³J. S. Lee, S. J. Moon, T. W. Noh, S. Nakatsuji, and Y. Maeno, *Phys. Rev. Lett.* **96**, 057401 (2006).
- ⁴B. J. Kim, J. Yu, H. Koh, I. Nagai, S. I. Ikeda, S.-J. Oh, and C. Kim, *Phys. Rev. Lett.* **97**, 106401 (2006).
- ⁵A. Shimoyamada, K. Ishizaka, S. Tsuda, S. Nakatsuji, Y. Maeno, and S. Shin, *Phys. Rev. Lett.* **102**, 086401 (2009).
- ⁶M. Neupane, P. Richard, Z.-H. Pan, Y.-M. Xu, R. Jin, D. Mandrus, X. Dai, Z. Fang, Z. Wang, and H. Ding, *Phys. Rev. Lett.* **103**, 097001 (2009).
- ⁷V. I. Anisimov, I. A. Nekrasov, D. E. Kondakov, T. M. Rice, and M. Sigríst, *Eur. Phys. J. B* **25**, 191 (2002).
- ⁸A. Koga, N. Kawakami, T. M. Rice, and M. Sigríst, *Phys. Rev. Lett.* **92**, 216402 (2004).
- ⁹C. Knecht, N. Blümer, and P. G. J. van Dongen, *Phys. Rev. B* **72**, 081103 (2005).
- ¹⁰A. Koga, N. Kawakami, T. M. Rice, and M. Sigríst, *Phys. Rev. B* **72**, 045128 (2005).
- ¹¹R. Arita and K. Held, *Phys. Rev. B* **72**, 201102 (2005).
- ¹²Y. Song and L.-J. Zou, *Phys. Rev. B* **72**, 085114 (2005).
- ¹³M. Ferrero, F. Becca, M. Fabrizio, and M. Capone, *Phys. Rev. B* **72**, 205126 (2005).
- ¹⁴L. de' Medici, A. Georges, and S. Biermann, *Phys. Rev. B* **72**, 205124 (2005).
- ¹⁵S. Biermann, L. de' Medici, and A. Georges, *Phys. Rev. Lett.* **95**, 206401 (2005).
- ¹⁶A. Liebsch, *Phys. Rev. Lett.* **95**, 116402 (2005).
- ¹⁷K. Inaba and A. Koga, *Phys. Rev. B* **73**, 155106 (2006).
- ¹⁸T. A. Costi and A. Liebsch, *Phys. Rev. Lett.* **99**, 236404 (2007).
- ¹⁹K. Bouadim, G. G. Batrouni, and R. T. Scalettar, *Phys. Rev. Lett.* **102**, 226402 (2009).
- ²⁰E. Jakobi, N. Blümer, and P. van Dongen, *Phys. Rev. B* **80**, 115109 (2009).
- ²¹Y. Song and L.-J. Zou, *Eur. Phys. J. B* **72**, 59 (2009).
- ²²H. Lee, Y.-Z. Zhang, H. O. Jeschke, R. Valentí, and H. Monien, *Phys. Rev. Lett.* **104**, 026402 (2010).
- ²³L. de' Medici, *Phys. Rev. B* **83**, 205112 (2011).
- ²⁴T. Kita, T. Ohashi, and N. Kawakami, *Phys. Rev. B* **84**, 195130 (2011).
- ²⁵S. Nakatsuji and Y. Maeno, *Phys. Rev. Lett.* **84**, 2666 (2000).
- ²⁶Z. Fang, N. Nagaosa, and K. Terakura, *Phys. Rev. B* **69**, 045116 (2004).
- ²⁷A. Liebsch and H. Ishida, *Phys. Rev. Lett.* **98**, 216403 (2007).
- ²⁸E. Gorelov, M. Karolak, T. O. Wehling, F. Lechermann, A. I. Lichtenstein, and E. Pavarini, *Phys. Rev. Lett.* **104**, 226401 (2010).
- ²⁹P. Werner and A. J. Millis, *Phys. Rev. Lett.* **99**, 126405 (2007).
- ³⁰L. de' Medici, S. R. Hassan, M. Capone, and X. Dai, *Phys. Rev. Lett.* **102**, 126401 (2009); L. de' Medici, S. R. Hassan, and M. Capone, *J. Supercond. Nov. Magn.* **22**, 535 (2009).
- ³¹H. Lee, Y.-Z. Zhang, H. O. Jeschke, and R. Valentí, *Phys. Rev. B* **84**, 020401(R) (2011).
- ³²W.-G. Yin, C.-C. Lee, and W. Ku, *Phys. Rev. Lett.* **105**, 107004 (2010).
- ³³Y.-Z. You, F. Yang, S.-P. Kou, and Z.-Y. Weng, *Phys. Rev. Lett.* **107**, 167001 (2011).
- ³⁴A. Hackl and M. Vojta, *New J. Phys.* **11**, 055064 (2009).
- ³⁵S.-P. Kou, T. Li, and Z.-Y. Weng, *EPL* **88**, 17010 (2009).
- ³⁶F. Yang, S.-P. Kou, and Z.-Y. Weng, *Phys. Rev. B* **81**, 245130 (2010).
- ³⁷Y.-Z. You, F. Yang, S.-P. Kou, and Z.-Y. Weng, *Phys. Rev. B* **84**, 054527 (2011).
- ³⁸W. Lv, F. Krüger, and P. Phillips, *Phys. Rev. B* **82**, 045125 (2010).
- ³⁹J. Wu, P. Phillips, and A. H. Castro Neto, *Phys. Rev. Lett.* **101**, 126401 (2008).
- ⁴⁰J. Lorenzana, G. Seibold, C. Ortix, and M. Grilli, *Phys. Rev. Lett.* **101**, 186402 (2008).
- ⁴¹M. Daghofer, A. Moreo, J. A. Riera, E. Arrigoni, D. J. Scalapino, and E. Dagotto, *Phys. Rev. Lett.* **101**, 237004 (2008).
- ⁴²E. Kaneshita, T. Morinari, and T. Tohyama, *Phys. Rev. Lett.* **103**, 247202 (2009).
- ⁴³E. Bascones, M. J. Calderón, and B. Valenzuela, *Phys. Rev. Lett.* **104**, 227201 (2010).
- ⁴⁴A. Georges, G. Kotliar, W. Krauth, and M. J. Rozenberg, *Rev. Mod. Phys.* **68**, 13 (1996).
- ⁴⁵G. Kotliar, S. Y. Savrasov, K. Haule, V. S. Oudovenko, O. Parcollet, and C. A. Marianetti, *Rev. Mod. Phys.* **78**, 865 (2006).
- ⁴⁶E. Gull, A. J. Millis, A. I. Lichtenstein, A. N. Rubtsov, M. Troyer, and P. Werner, *Rev. Mod. Phys.* **83**, 349 (2011).
- ⁴⁷H. Lee, Y.-Z. Zhang, H. O. Jeschke, and R. Valentí, *Phys. Rev. B* **81**, 220506(R) (2010).
- ⁴⁸R. Peters and T. Pruschke, *Phys. Rev. B* **79**, 045108 (2009).
- ⁴⁹Z.-Q. Yu and L. Yin, *Phys. Rev. B* **81**, 195122 (2010).
- ⁵⁰S. Raghu, X.-L. Qi, C.-X. Liu, D. J. Scalapino, and S.-C. Zhang, *Phys. Rev. B* **77**, 220503 (2008).
- ⁵¹A. Akbari, I. Eremin, and P. Thalmeier, *Phys. Rev. B* **84**, 134513 (2011).
- ⁵²C. Zhang, M. Wang, H. Luo, M. Wang, M. Liu, J. Zhao, D. L. Abernathy, K. Marty, M. D. Lumsden, S. Chi, S. Chang, J. A. Rodriguez-Rivera, J. W. Lynn, T. Xiang, J. Hu, and P. Dai, *Sci. Rep.* **1**, 115 (2011).
- ⁵³H. Q. Yuan, L. Jiao, F. F. Balakirev, J. Singleton, C. Setty, J. P. Hu, T. Shang, L. J. Li, G. H. Cao, Z. A. Xu, B. Shen, and H. H. Wen, e-print [arXiv:1102.5476v1](https://arxiv.org/abs/1102.5476v1).